

On The Performance of Equalization Techniques for Aeronautical Telemetry

Michael Rice
Brigham Young University
Provo, UT 84602

Mohammad Saquib
Md. Shah Afran
The University of Texas at Dallas
Richardson, TX 75083

Arlene Cole-Rhodes
Farzad Moazzami
Morgan State University
Baltimore, MD 21251

Abstract—This paper compares the performance of the zero-forcing (ZF), minimum mean-squared error (MMSE), and MMSE-initialized CMA+AMA equalizers using SOQPSK-TG over multipath channels captured during channel sounding experiments at Edwards AFB. The ZF and MMSE equalizers are data-aided and are based on estimates of the channel conditions derived from the preamble and ASM bits included in each iNET packet. The simulated bit error rate results show that MMSE and CMA+AMA achieve similar performance and are both about 1–3 dB better than the ZF equalizer. Comparison with the optimum AWGN detector shows that 4–9 dB of link margin is required to account for the multipath interference.

I. INTRODUCTION

Over the past several decades, the increasing complexity of air-borne test articles has pushed telemetry data rates higher and higher. The higher data rates have increased the bandwidth of the modulated carrier to the point where multipath fading is no longer frequency non-selective, but frequency selective. Consequently, multipath interference is now the dominant cause of link outages in aeronautical telemetry.

The traditional solutions are spatial diversity and/or equalization. The high costs of transmit and/or receive diversity push the system designer in the direction of equalization. Equalization, as a technique to overcome inter-symbol interference (ISI) due to multipath propagation (or other causes), has been well-studied (see, for example, Chapters 9 and 10 of [1]). Because the modulations used in aeronautical telemetry (PCM/FM and SOQPSK-TG) are nonlinear continuous phase modulations (CPMs), direct application of the traditional equalization techniques to the data symbols is not possible. But both modulations are constant modulus. For this reason blind, adaptive CMA algorithm that has received most of the attention in aeronautical telemetry applications [2], [3], [4], [5]. The somewhat ambiguous results did not inspire widespread adoption of this equalization algorithm.

Here we investigate the performance of data-aided equalization techniques. By leveraging the presence of known data symbols (in the form of the iNET preamble and ASM bits), an estimate of the channel conditions is used to design “better

This work was funded by the Test Resource Management Center (TRMC) Test and Evaluation Science and Technology (T&E/S&T) Program through the U.S. Army Program Executive Office for Simulation, Training and Instrumentation (PEO STRI) under contract W900KK-13-C-0026 (PAQ). Approved for public release; distribution is unlimited. 412TW-PA-14241.

PRE (128 bits)	ASM (64 bits)	DATA (6144 bits)
-------------------	------------------	---------------------

Fig. 1. The iNET packet structure used in this paper.

informed” equalizers. Here we compare the performance of the zero-forcing (ZF), minimum mean-squared error (MMSE), and MMSE-initialized CMA+AMA equalizers over multipath channels captured during channel sounding experiments at Edwards AFB. In the following \mathbf{M}^T and \mathbf{M}^\dagger denote the transpose and conjugate transpose (“Hermitian”), respectively, of the matrix \mathbf{M} .

II. SIGNAL MODEL AND ESTIMATORS

The bit sequence for iNET is organized as outlined in the top portion of Figure 1. The preamble sequence (PRE) is CD98_{hex} repeated eight times [6, p. 48]. The attached sync marker (ASM) field is 034776C7272895B0_{hex}. The DATA field is 6144 randomized data bits. (These bits correspond to a single LDPC codeword in the coded system. Here, we evaluate the uncoded bit error rate after equalization.)

The transmitted signal, $s(t)$, is SOQPSK-TG whose input bit stream is summarized in Figure 1. SOQPSK-TG is a partial response CPM waveform with a constrained ternary alphabet. The details are spelled out in [7], [8]. The signal propagates through a frequency selective channel and experiences a frequency offset as well as the addition of additive white Gaussian noise.

The received signal is filtered, down-converted to complex baseband, and sampled (not necessarily in that order) using standard techniques. The resulting sequence of received samples is

$$r(n) = \left[\sum_{k=-N_1}^{N_2} h(k)s(n-k) \right] e^{j\omega_0 n} + w(n), \quad (1)$$

where $h(n)$ is the impulse response of the equivalent discrete-time channel with support on $-N_1 \leq n \leq N_2$, ω_0 rads/sample is the frequency offset, and $w(n)$ is a proper [9] complex-valued zero-mean Gaussian random process with auto-covariance function

$$\frac{1}{2} \mathbb{E} \{ w(n)w^*(n-k) \} = \sigma_w^2 \delta(k). \quad (2)$$

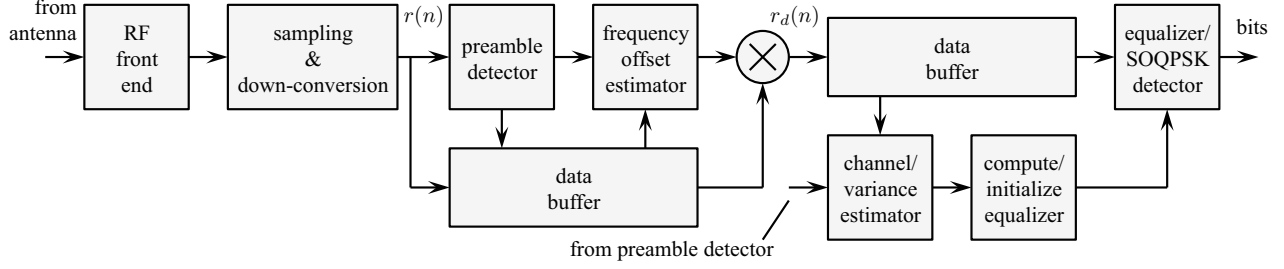


Fig. 2. The data packet format and high-level signal processing explored in this paper.

Because SOQPSK-TG is a nonlinear modulation, the equalizer cannot operate on the symbols in the same way it does for linear modulation (cf., [1, Chapter 9]). Consequently, the equalizer must operate on the samples of SOQPSK-TG, similar to the way fractionally spaced equalizers operate.

Because the preamble and ASM bits are known, the samples corresponding to the preamble and ASM bits are used to estimate the frequency offset, channel impulse response, and, for the MMSE equalizer, the noise variance. Before these tasks can be accomplished, the start of the samples corresponding to the preamble bits in the received signal must be known. This is accomplished by the preamble detector block, whose algorithm is based on the detection algorithm described in [10]. Once the start of the preamble is known, the frequency offset is estimated using the D&M estimator described in [11]. The frequency offset estimate is used with a complex-exponential to derotate the received data to remove the frequency offset.

The derotated data $r_d(n)$ are used to estimate the channel and noise variance using the standard maximum likelihood (ML) technique. Let i be the index in $r(n)$ corresponding to the beginning of the preamble sequence and let L_p be the number of samples in the preamble sequence and L_a the number of samples in the ASM sequence. Define \mathbf{r} as the $(N_p + N_a - N_1 - N_2) \times 1$ vector formed from the samples of the received signal corresponding to preamble and ASM fields¹ but skipping the first N_2 samples and last N_1 samples:

$$\mathbf{r} = \begin{bmatrix} r(i + N_2) \\ \vdots \\ r(i + N_p + N_{asm} - N_1 - 1) \end{bmatrix}. \quad (3)$$

This vector is related to the samples corresponding to the preamble and ASM samples, the channel, and the noise as follows: Let $x(0), x(1), \dots, x(L_p + L_a - 1)$ be the samples of the SOQPSK-TG signal corresponding to the preamble and ASM fields and let \mathbf{X} be the $(N_p + N_a - N_1 - N_2) \times (N_1 + N_2 + 1)$

convolution matrix formed from these samples:

$$\begin{bmatrix} x(N_2 + N_1) & \cdots & x(0) \\ \vdots & & \vdots \\ x(N_p + N_a - 1) & \cdots & x(N_p + N_a - N_1 - N_2 - 1) \end{bmatrix}.$$

Let \mathbf{h} be the $(N_1 + N_2 + 1) \times 1$ vector formed by the channel coefficients,

$$\mathbf{h} = [h(-N_1) \quad \cdots \quad h(N_2)]^T, \quad (4)$$

and let \mathbf{w} be the $(N_p + N_a - N_1 - N_2) \times 1$ vector of noise samples. Then

$$\mathbf{r} = \mathbf{X}\mathbf{h} + \mathbf{w}. \quad (5)$$

The conditional probability density function (PDF) of \mathbf{r} is

$$f(\mathbf{r}|\mathbf{h}, \sigma_w^2) = \frac{1}{(2\pi\sigma_w^2)^L} \exp \left\{ -\frac{1}{2\sigma_w^2} |\mathbf{r} - \mathbf{X}\mathbf{h}|^2 \right\}, \quad (6)$$

where $L = N_p + N_a - N_1 - N_2$. The log-likelihood function for \mathbf{h} and σ_w^2 is

$$\Lambda(\mathbf{h}, \sigma_w^2) = -L \log(2\pi\sigma_w^2) - \frac{1}{2\sigma_w^2} |\mathbf{r} - \mathbf{X}\mathbf{h}|^2 \quad (7)$$

from which the ML estimates² are

$$\hat{\mathbf{h}} = (\mathbf{X}^\dagger \mathbf{X})^{-1} \mathbf{X}^\dagger \mathbf{r}. \quad (8)$$

$$\hat{\sigma}_w^2 = \frac{1}{2\rho} |\mathbf{r} - \mathbf{X}\hat{\mathbf{h}}|^2 \quad (9)$$

where

$$\rho = \text{Tr} \left\{ \mathbf{I}_L - \mathbf{X} (\mathbf{X}^\dagger \mathbf{X})^{-1} \mathbf{X}^\dagger \right\} \quad (10)$$

where \mathbf{I}_L is the $L \times L$ identity matrix.

III. EQUALIZATION TECHNIQUES

The zero-forcing (ZF) and minimum mean squared error (MMSE) equalizers operate in the system shown in Figure 3 (cf., Figure 2). Here, the derotated samples $r_d(n)$ are equalized using a length $L_1 + L_2 + 1$ FIR filter defined by the impulse response $c(n)$ for $-L_1 \leq n \leq L_2$ to produce the output

$$y(n) = \sum_{m_1=-L_1}^{L_2} c(m_1) r_d(n - m_1). \quad (11)$$

¹Because the preamble is an 8-times repetition of CD98_{hex}, the convolution matrix formed from the samples corresponding to the preamble is not sufficiently well-conditioned to provide robust channel estimates in the presence of even a small frequency offset. The convolution matrix formed from samples corresponding to both the preamble and ASM fields has less structure and provides more robust channel estimates. See Section 4 of [12].

²The ML estimator for the noise variance is $|\mathbf{r} - \mathbf{X}\hat{\mathbf{h}}|^2/(2L)$ and is *biased*. The noise variance estimator (9) is not the ML estimate, but rather the *unbiased* estimator motivated by the ML estimator. See Section 7 of [12].

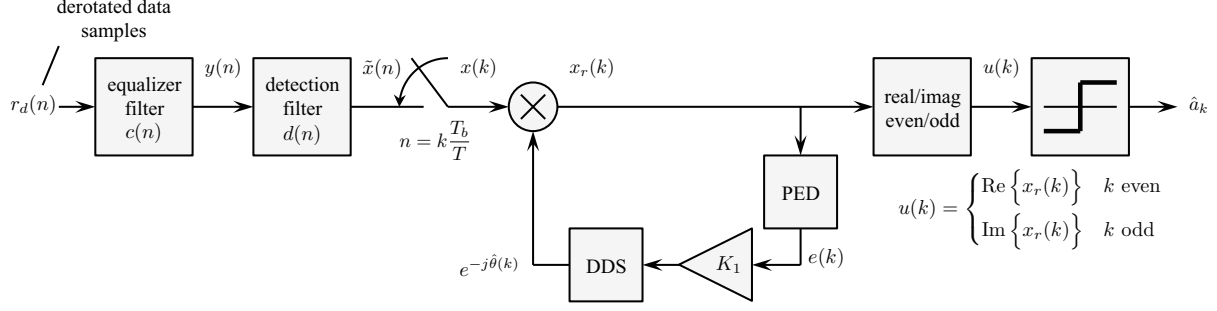


Fig. 3. A block diagram of the system used for the ZF and MMSE equalizers.

The equalizer output forms the input to the symbol-by-symbol SOQPSK detector comprising a detection filter operating at $N = T_b/T$ samples/bit and a decision process, operating on the decision variable $u(k)$ at 1 sample/bit. This detector, based on the an offset QPSK approximation of SOQPSK-TG, is described in more detail in [7], [8]. The detection filter output is

$$\tilde{x}(n) = \sum_{m_2=-L_d}^{L_d} d(m_2)y(n-m_2) \quad (12)$$

and the downsampled detection filter output is, for $N = 2$ samples/bit

$$x(k) = \tilde{x}(2k). \quad (13)$$

The phase compensated (rotated) samples are

$$x_r(k) = e^{-j\hat{\theta}(k)}x(k). \quad (14)$$

Finally, the decision variables $u(k)$ are formed as shown in Figure 3.

The detector of Figure 3 also includes a phase lock loop (PLL). The PLL is required to track out any residual phase increments due to frequency offset estimation errors. A timing loop is not required because timing offsets are part of the channel estimated by (8).

A. ZF Equalizer

The zero-forcing equalizer is a filter that is the best length- $(L_1 + L_2 + 1)$ FIR approximation to the “inverse” of the channel. That is, $c(n)$ is chosen so that

$$\hat{h}(n) * c(n) \approx \delta(n - n_0) \quad (15)$$

for $-L_1 \leq n \leq L_2$ where “best” minimizes the least squares error. The vector of filter coefficients defined by this criterion is given by [13]

$$\mathbf{c}_{ZF} = (\mathbf{H}^\dagger \mathbf{H})^{-1} \mathbf{H}^\dagger \mathbf{u}_{n_0} \quad (16)$$

where

$$\mathbf{u}_{n_0} = \begin{bmatrix} 0 \\ \vdots \\ 0 \\ 1 \\ 0 \\ \vdots \\ 0 \end{bmatrix} \left\{ \begin{array}{l} n_0 - 1 \text{ zeros} \\ N_1 + N_2 + L_1 + L_2 - n_0 + 1 \text{ zeros} \end{array} \right.$$

and \mathbf{H} is the $(N_1 + N_2 + L_1 + L_2 + 1) \times (L_1 + L_2 + 1)$ convolution matrix formed by the estimates of the channel impulse response:

$$\mathbf{H} = \begin{bmatrix} \hat{h}(-N_1) & & & \\ \hat{h}(-N_1+1) & \hat{h}(-N_1) & & \\ \vdots & \vdots & \ddots & \\ \hat{h}(N_2) & \hat{h}(N_2-1) & \hat{h}(N_2) & \hat{h}(-N_1) \\ & \hat{h}(N_2) & \hat{h}(-N_1+1) & \\ & & \vdots & \hat{h}(N_2) \end{bmatrix}.$$

B. MMSE Equalizer

The minimum mean-squared error (MMSE) equalizer is a filter that minimizes the mean squared error

$$\mathcal{E} = \mathbb{E} \left\{ \left| s(n) - r(n) * c(n) \right|^2 \right\}. \quad (17)$$

The solution is given by a form of the Wiener-Hopf equations [13]. The MMSE equalizer filter coefficients are

$$\mathbf{c}_{MMSE} = \left[\mathbf{G} \mathbf{G}^\dagger + \frac{\hat{\sigma}_w^2}{\hat{\sigma}_s^2} \mathbf{I}_{L_1+L_2+1} \right]^{-1} \mathbf{g}^\dagger, \quad (18)$$

where \mathbf{G} is the $(L_1 + L_2 + 1) \times (N_1 + N_2 + L_1 + L_2 + 1)$ matrix

$$\mathbf{G} = \begin{bmatrix} \hat{h}(N_2) & \cdots & \hat{h}(-N_1) & & \\ & \hat{h}(N_2) & \cdots & \hat{h}(-N_1) & \\ & & \ddots & & \\ & & & \hat{h}(N_2) & \cdots & \hat{h}(-N_1) \end{bmatrix};$$

\mathbf{g} is the $1 \times (L_1 + L_2 + 1)$ vector given by

$$\mathbf{g} = [\hat{h}(L_1) \quad \cdots \quad \hat{h}(-L_2)]$$

where it is understood that $h(n) = 0$ for $n < -N_1$ or $n > N_2$ (how many zeros need to be prepended and appended depends on the relationship between L_1 and N_2 and the relationship between L_2 and N_1); and

$$\sigma_s^2 = \frac{1}{2} \mathbb{E} \left\{ |s(n)|^2 \right\} \quad (19)$$

is the signal power. This solution is based on the assumption that SOQPSK-TG samples corresponding to a sample rate of 2 samples/bit are approximately uncorrelated. The impact of this approximation is discussed in [14].

C. CMA+AMA Equalizer

The CMA+AMA equalizer investigated in this paper is an extension of a similar idea described in [15] and is outlined in Figure 4. As with the ZF and MMSE equalizers of Figure 3, the length- $(L_1 + L_2 + 1)$ FIR equalizer filter precedes the SOQPSK-TG symbol-by-symbol detector. Unlike the ZF and MMSE equalizers of Figure 3, the CMA+AMA equalizer is an adaptive filter whose coefficients minimize the cost function

$$J = J_{\text{CMA}} + \beta J_{\text{AMA}} \quad (20)$$

for a weighting constant $\beta \geq 0$. The costs functions are

$$J_{\text{CMA}}(y(n)) = \mathbb{E} \left\{ \left(|y(n)|^2 - R_2 \right)^2 \right\} \quad (21)$$

where

$$R_2 = \frac{\mathbb{E} \left\{ |s(n)|^4 \right\}}{\mathbb{E} \left\{ |s(n)|^2 \right\}}, \quad (22)$$

and

$$J_{\text{AMA}}(u(k)) = \mathbb{E} \left\{ 1 - \sum_{a \in \mathcal{C}} \exp \left[-\frac{1}{2\sigma^2} |u(k) - a|^2 \right] \right\} \quad (23)$$

where \mathcal{C} is the set of constellation points

$$\mathcal{C} = \left\{ -A - jA, -A + jA, +A - jA, +A + jA \right\}. \quad (24)$$

The CMA cost function measures the departure of the equalizer output from a circle of radius R_2 , but does so without any phase information. Consequently, some form of blind phase alignment is needed. The phase alignment (up to a $\pi/2$ phase ambiguity) is provided by the AMA cost function, that measures the departure of the decision variable from the four constellation points. We note that because SOQPSK-TG is only approximately an offset QPSK, J_{AMA} is orders of magnitude larger than J_{CMA} , even under ideal conditions. For this reason, the weighting parameter β must be carefully chosen.

Using the steepest descent algorithm to drive the adaptation, which occurs once per packet here, the $(L_1 + L_2 + 1) \times 1$ vector

of filter coefficients for packet $b + 1$ is an updated version of the filter coefficients used for packet b :

$$\mathbf{c}_{b+1} = \mathbf{c}_b - \mu \left(\nabla J_{\text{CMA}} + \beta \nabla J_{\text{AMA}} \right) \quad (25)$$

where $\mu > 0$ is the step size and where

$$\nabla J_{\text{CMA}} = \mathbb{E} \left\{ 2 \left[y(n)y^*(n) - R_2 \right] y(n) \mathbf{r}^*(n) \right\} \quad (26)$$

with

$$\mathbf{r}^*(n) = \begin{bmatrix} r_d^*(n + L_1) \\ \vdots \\ r_d^*(n) \\ \vdots \\ r_d^*(n - L_2) \end{bmatrix}, \quad (27)$$

and where

$$\nabla J_{\text{AMA}} = \mathbb{E} \left\{ \sum_{a \in \mathcal{C}} \exp \left[-\frac{1}{2\sigma^2} |u(k) - a|^2 \right] \frac{1}{2\sigma^2} [u(k) - a] \times \mathbf{D} \left(\mathbf{r}_R(4k) - j\mathbf{r}_I(4k + 2) \right) \right\} \quad (28)$$

where \mathbf{D} is the $(L_1 + L_2 + 1) \times (2L_d + L_1 + L_2)$ convolution matrix formed from the detection filter impulse response

$$\mathbf{D} = \begin{bmatrix} d(-L_d) & \cdots & d(L_d) & & \\ & \ddots & & & \\ & & d(-L_d) & \cdots & d(L_d) \\ & & & \ddots & \\ & & & & d(-L_d) & \cdots & d(L_d) \end{bmatrix}$$

and where, using the notation $r_d(n) = r_R(n) + jr_I(n)$,

$$\mathbf{r}_R = \begin{bmatrix} r_R(4k + L_d + L_1) \\ \vdots \\ r_R(4k) \\ \vdots \\ r_R(4k - L_d - L_2) \end{bmatrix} \quad \mathbf{r}_I = \begin{bmatrix} r_I(4k + 2 + L_d + L_1) \\ \vdots \\ r_I(4k + 2) \\ \vdots \\ r_I(4k + 2 - L_d - L_2) \end{bmatrix}.$$

IV. RESULTS AND CONCLUSIONS

The bit error rate (BER) performance of the three equalization algorithms over three representative channels, derived from channel sounding measurements conducted at Edwards AFB [16], was evaluated in computer simulation. These channels are illustrated in Figure 5. See the figure caption for more details. In these simulations, the iNET preamble and ASM fields were used with SOQPSK-TG operating at 10.3125 Mibts/s (the “over-the-air” bit rate corresponding to a “payload” bit rate of 10 Mibts/s). The following simulation parameters were used:

- The SOQPSK-TG signal and channel were sampled at a rate equivalent to 2 samples/bit.
- Ideal preamble synchronization was used.
- The D&M frequency offset estimator described in [11] was used to estimate the frequency offset and derotate the data as described in Figure 2.

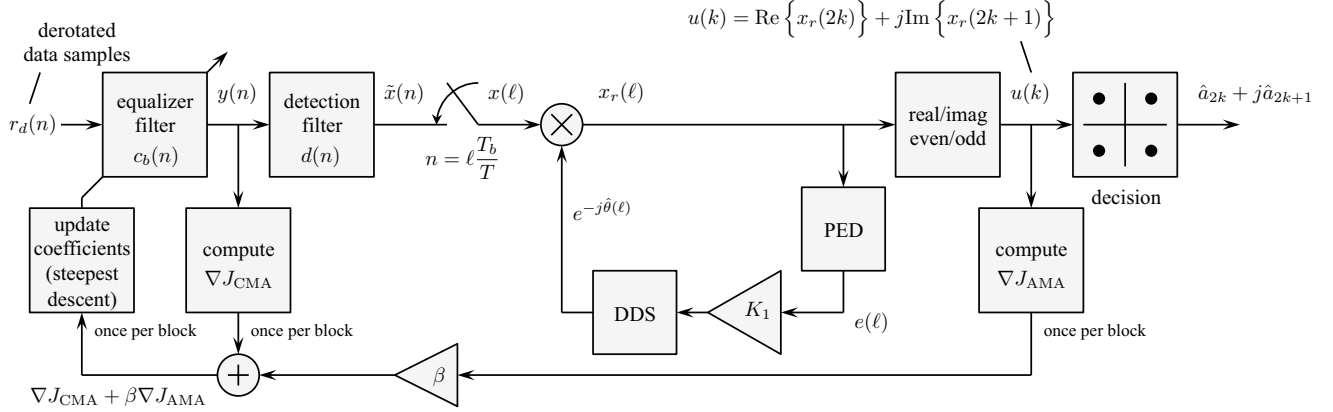


Fig. 4. A block diagram of the system used for the CMA+AMA equalizer.

- The channel estimator (8) used $N_1 = 12$ and $N_2 = 25$ for all three channels.
- The equalizers used $L_1 = 4 \times N_1$ and $L_2 = 4 \times N_2$.
- For the MMSE equalizer coefficients, the noise variance estimate (9) was used in (18).
- For the CMA+AMA equalizer, the step size μ in the update (25) was set to 5×10^{-3} .

For the ZF and MMSE equalizers, the channel impulse response was estimated anew for each occurrence of the preamble and ASM fields. The equalizer filter coefficients were computed from the channel impulse response estimate and remained fixed for the duration of the corresponding packet.

For the CMA+AMA equalizer, convergence was aided by initializing the equalizer filter with the MMSE filter coefficients. The adaptive filter was allowed to converge for 100 packets before errors were counted. The expectations in (26) and (28) were estimated using the sample means for the data over an entire packet. Based on the authors' experience with multiple simulations, the MMSE initialization rendered unnecessary the AMA error function. Consequently, $\beta = 0$ for the simulations presented below.

The BER simulation results are shown in Figures 6 – 8. Here we observe that the MMSE and CMA+AMA equalizers have very similar performance, and are about 1–3 dB better than the ZF equalizer. Also included in the plots is the performance of the optimum detector for SOQPSK-TG (a sequence detector based on the Viterbi algorithm [7], [8]) in AWGN. The performance of the MMSE and CMA+AMA equalizers is about 4–9 dB worse over the range of E_b/N_0 and the three channels examined here. This gives a sense of the additional link margin required to accommodate data-aided equalization over these channels.

REFERENCES

- [1] J. Proakis and M. Salehi, *Digital Communications*, 5th ed. New York: McGraw-Hill, 2008.
- [2] Z. Ye, E. Satorius, and T. Jedrey, "Enhancement of advanced range telemetry (ARTM) channels via blind equalization," in *Proceedings of*

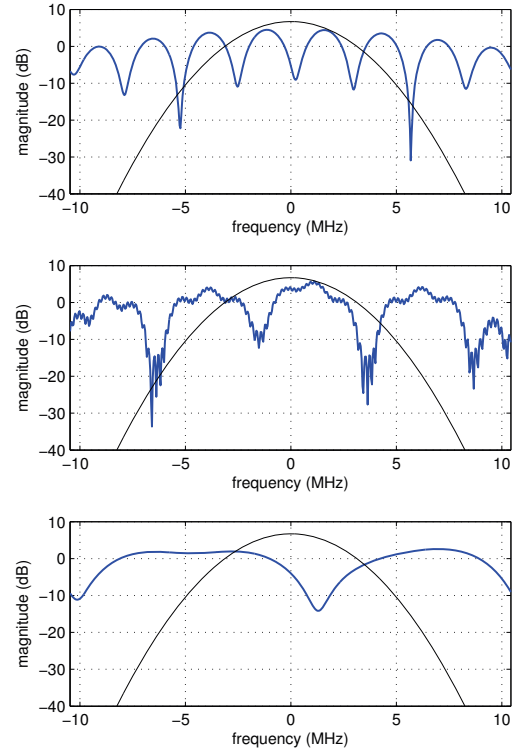


Fig. 5. The example channels from channel sounding experiments at Edwards AFB: (top) a length-9 channel from the flight line; (middle) a length-19 channel from take-off; (bottom) a length-5 channel from low-elevation angle "up and away" flight. In each plot, the thick line is the channel frequency response and the thin line is the power spectral density of SOQPSK-TG operating at 10.3125 Mbits/s.

the *International Telemetry Conference*, Las Vegas, NV, October 2001.

- [3] T. Hill and M. Geoghegan, "A comparison of adaptively equalized PCM/FM, SOQPSK, and multi-h CPM in a multipath channel," in *Proceedings of the International Telemetry Conference*, San Diego, CA, October 2002.
- [4] M. Geoghegan, "Experimental results for PCM/FM, Tier I SOQPSK, and Tier II Multi-h CPM with CMA equalization," in *Proceedings of the International Telemetry Conference*, Las Vegas, NV, October 2003.

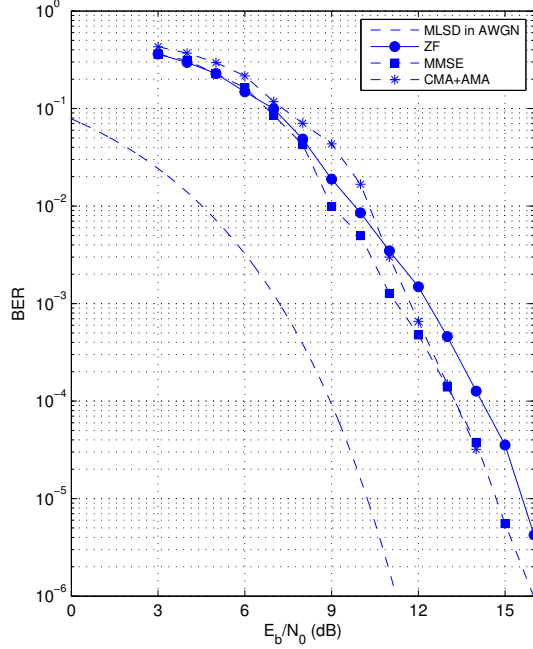


Fig. 6. Equalized BER simulations for the ZF, MMSE, and CMA+AMA equalizers for the first channel of Figure 5.

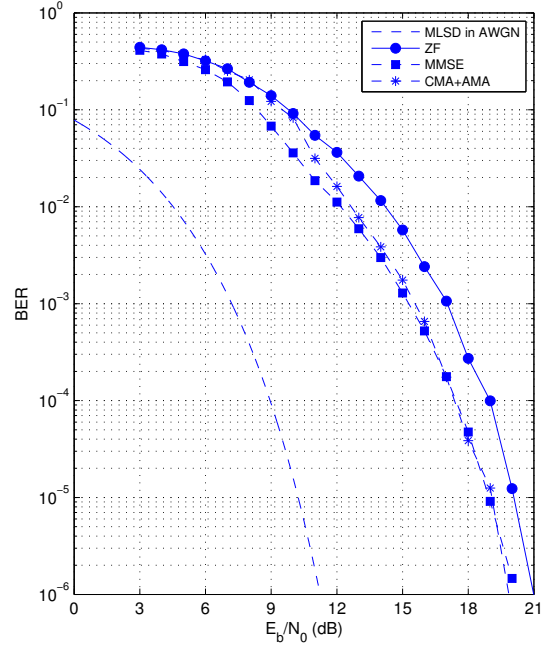


Fig. 8. Equalized BER simulations for the ZF, MMSE, and CMA+AMA equalizers for the third channel of Figure 5.

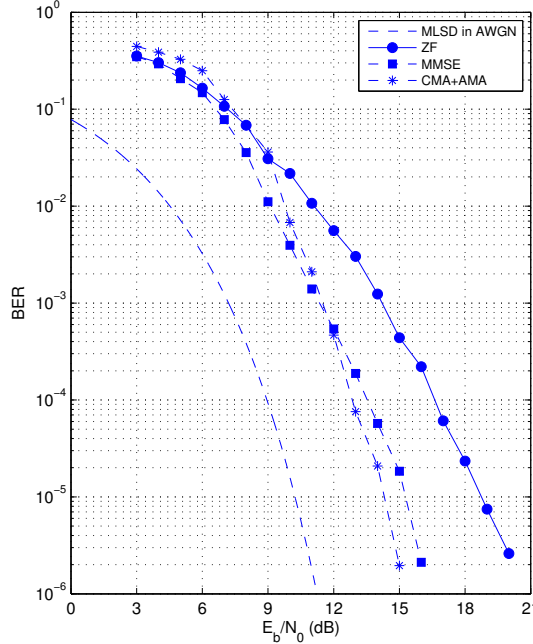


Fig. 7. Equalized BER simulations for the ZF, MMSE, and CMA+AMA equalizers for the second channel of Figure 5.

- [5] E. Law, "How well does a blind adaptive CMA equalizer work in a simulated telemetry multipath environment?" in *Proceedings of the International Telemetry Conference*, San Diego, CA, October 2004.
- [6] Integrated Network Enhanced Telemetry (iNET) Radio Access Network Standards Working Group, "Radio access network (RAN) standard, version 0.7.9," Tech. Rep., available at <https://www.tena-sda.org/display/INET/iNET+Platform+Interface+Standards>.
- [7] T. Nelson, E. Perrins, and M. Rice, "Near optimal common detection techniques for shaped offset QPSK and Feher's QPSK," *IEEE Transactions on Communications*, vol. 56, no. 5, pp. 724–735, May 2008.
- [8] E. Perrins, "FEC systems for aeronautical telemetry," *IEEE Transactions on Aerospace and Electronic Systems*, vol. 49, no. 4, pp. 2340–2352, October 2013.
- [9] P. Schreier and L. Scharf, *Statistical Signal Processing of Complex-Valued Data*. New York: Cambridge University Press, 2010.
- [10] M. Rice and A. McMurdie, "A preamble detector for iNET-formatted bursts using SOQPSK," in *Proceedings of the IEEE Military Communications Conference*, Baltimore, MD, November 2014.
- [11] M. Rice and E. Perrins, "On frequency offset estimation using the iNET preamble in frequency selective fading channels," in *Proceedings of the IEEE Military Communications Conference*, Baltimore, MD, November 2014.
- [12] M. Rice, "Phase 1 report: Preamble assisted equalization for aeronautical telemetry (PAQ)," Brigham Young University, Tech. Rep., 2014, submitted to the Spectrum Efficient Technologies (SET) Office of the Science & Technology, Test & Evaluation (S&T/T&E) Program, Test Resource Management Center (TRMC). Also available on-line at <http://hdl.lib.byu.edu/1877/3242>.
- [13] M. Hayes, *Statistical Digital Signal Processing and Modeling*. New York: John Wiley & Sons, 1996.
- [14] M. Rice, M. S. Afran, and M. Saquib, "Equalization in aeronautical telemetry using multiple antennas," in *Proceedings of the IEEE Military Communications Conference*, Baltimore, MD, November 2014.
- [15] A. Beasley and A. Cole-Rhodes, "Performance of an adaptive blind equalizer for QAM signals," in *Proceedings of the IEEE Military Communications Conference*, Atlantic City, NJ, October 2005.
- [16] M. Rice and M. Jensen, "A comparison of L-band and C-band multipath propagation at Edwards AFB," in *Proceedings of the International Telemetry Conference*, Las Vegas, NV, October 2011.